Inverted organic solar cells based on aqueous processed ZnO interlayers at low temperature

Sai Bai, Zhongwei Wu, Xiaoli Xu, Yizheng Jin, Baoquan Sun et al.

Citation: Appl. Phys. Lett. **100**, 203906 (2012); doi: 10.1063/1.4719201
View online: http://dx.doi.org/10.1063/1.4719201
View Table of Contents: http://apl.aip.org/resource/1/APPLAB/v100/i20
Published by the American Institute of Physics.

Inverted organic solar cells based on aqueous processed ZnO interlayers at low temperature

Sai Bai,[1] Zhongwei Wu,[2] Xiaoli Xu,[3] Yizheng Jin,[1,a)] Baoquan Sun,[2,a)] Xiaojun Guo,[3,a)] Shasha He,[1] Xin Wang,[1] Zhizhen Ye,[1] Huaixin Wei,[2] Xiaoyuan Han,[2] and Wanli Ma[2]
[1]*State Key Laboratory of Silicon Materials, Department of Materials Science and Engineering, Zhejiang University, Hangzhou 310027, People's Republic of China*
[2]*Jiangsu Key Laboratory for Carbon-Based Functional Materials & Devices, Institute of Functional Nano & Soft Materials (FUNSOM), Soochow University, 199 Ren'ai Road, Suzhou 215123, People's Republic of China*
[3]*Department of Electronic Engineering, Shanghai Jiao Tong University, 800 Dongchuan Rd., Shanghai 200240, People's Republic of China*

(Received 15 March 2012; accepted 29 April 2012; published online 18 May 2012)

A facile solution processable and low temperature ($\leq$150 °C) approach was developed to deposit ZnO electron transport interlayers for inverted organic solar cells. The ZnO thin films were fabricated from the stable and non-toxic aqueous precursor solutions of ammine-hydroxo zinc complex, $[Zn(NH_3)_x](OH)_2$. The resulting inverted poly (3-hexylthiophene): [6-6]-phenyl C_{61} butyric acid methyl ester solar cells exhibited power conversion efficiency of 4.17% as well as decent stability. We demonstrate that the work function of the ZnO electron transport interlayers was critical in terms of governing the photovoltaic performance of the inverted devices. © *2012 American Institute of Physics*. [http://dx.doi.org/10.1063/1.4719201]

Organic photovoltaics (OPVs) are considered as an attractive approach to low cost solar energy harvesting due to the possibility of employing high throughput printing and coating techniques and the compatibility with flexible plastic substrates.[1–4] Recent advances in polymer synthetic chemistry and device processing have led to OPVs with impressive power conversion efficiencies (PCEs) exceeding 8%.[5] However, device stability must be improved so that OPV may become a marketable technology.

The conventional device geometry of OPVs, which comprises a bottom indium tin oxide (ITO) anode modified by poly(3,4-ethylenedioxythiophene)-poly(styrene sulfonate) (PEDOT:PSS), a photoactive layer, and a low work-function metal cathode, has several drawbacks in terms of achieving long-term stability.[6] For instance, due to the hygroscopic and acidic nature of PEDOT: PSS, the ITO/PEDOT: PSS interface is not stable.[7] In order to address these problems, OPV devices with an inverted geometry, which utilize metal oxide interlayers with adequate work functions and band structures to modify the electrodes and break the symmetry, have been developed.[8–10] In general, inverted organic solar cells have shown improved stabilities and comparable PCEs to their conventional counterparts.[11–13] Therefore, the inverted structures are appealing for future large scale production of OPVs.[9]

Among the n-type electron transport oxides, ZnO is the most promising material owning to the low work function, high electron mobility, excellent optical transparency, and environmentally friendly nature. A number of techniques, such as *in-situ* sol-gel, use of colloidal nanoparticles, atomic layer deposition, electro-deposition, spray pyrolysis, and use of nanoparticle-polymer composites, were demonstrated to deposit ZnO electron transport interlayers onto the ITO electrodes.[10,13–17] In principle, the processing of the ZnO interlayers shall meet several criteria. First, the approach of depositing ZnO thin films should be solution processable in order to take advantage of the high throughput fabrication techniques. Second, a low processing temperature, i.e., $\leq$150 °C, is preferred so that the processing is compatible with flexible substrates. Third, the stock solution that contains either precursors of ZnO or colloidal nanoparticles should be stable for a reasonable period of time. Finally, an environmentally benign processing is highly desirable to reduce the hazards. We noticed that Keszler *et al*. reported a simple and green strategy to fabricate ZnO thin film transistors (TFTs) at low temperatures ($\leq$150 °C) by employing ammine-hydroxo zinc complex, $[Zn(NH_3)_x](OH)_2$, in aqueous solutions as precursor material.[18] In this regard, we propose that the aqueous precursor of ammine-hydroxo zinc complex, owning to the rapid, low activation energy kinetics of metal-ammine dissociation and hydroxide condensation/dehydration reactions, is ideal for the deposition of the ZnO electron transport interlayers at low temperatures. We fabricated inverted solar cells using the model system of poly (3-hexylthiophene) (P3HT) and [6-6]-phenyl C61 butyric acid methyl ester (PCBM) blends to verify our hypothesis. In additional, we analyzed the effects of UV-ozone treatment on the properties of ZnO electron transport interlayers and the overall performance of the inverted solar cells.

We prepared the precursor solution according to the literature report. A $Zn(OH)_2$ agglomerate was generated by reacting $Zn(NO_3)_2$ (Alfa Aesar, 99.998%) with NaOH (Alfa Aesar, 99.99%). Centrifugation and supernatant decantation steps were repeated four times to remove the counter ions of Na^+ and NO_3^-. After the final centrifugation, the hydrated precipitate was dissolved in 40 ml of 6.6 mol/l NH_3 (aq.) (Alfa Aesar, 99.99%), to form a stock precursor solution. The concentration of the $[Zn(NH_3)_x](OH)_2$ precursor solution, determined by inductively coupled plasma atomic

[a)]Authors to whom correspondence should be addressed. Electronic addresses: yizhengjin@zju.edu.cn, bqsun@suda.edu.cn, and x.guo@sjtu.edu.cn.

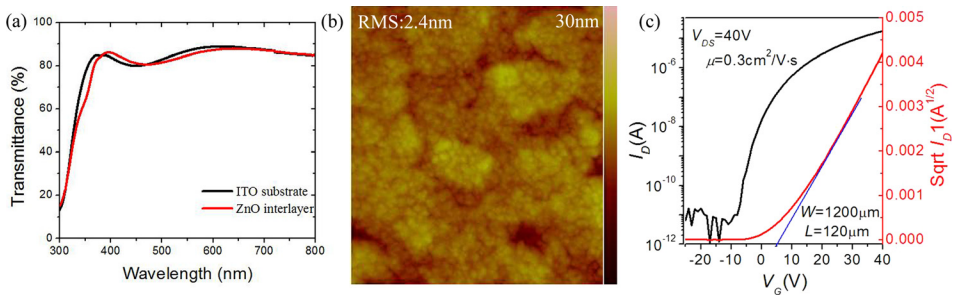

FIG. 1. (a) Transmission spectra of the ZnO interlayers deposited onto the ITO electrode which were annealed at 150 °C for 10 min in glove box and the ITO substrates. (b) An AFM image of the ZnO films from the aqueous precursor. (c) Transfer curve of TFTs based on the ZnO films from the aqueous precursor.

absorption spectrophotometer (ICP-AAS, Thermo Electron SOLAAR M6), was 0.15 mol/l. The stock precursor solution was stable at ambient conditions for a period of over six months.

The ZnO thin films were obtained by spin coating the aqueous precursor solution onto the cleaned ITO substrates, followed by annealing in glove box at 150 °C for 10 min. The optical, structural, and morphological features of the ZnO films were analyzed by UV-visible absorption spectrum (UV-Vis, Shimadzu, UV-3600) and atomic force microscopy (AFM, Veeco MultiMode V). As revealed by the optical transmittance spectra (Figure 1(a)), the ZnO thin films are highly transparent in the visible region. AFM measurements (Figure 1(b)) indicate that the root mean square (RMS) surface height of the ZnO films is about 2.4 nm. The transport properties of the ZnO thin films annealed at 150 °C were characterized by means of bottom-gate and top-contact TFTs. The extracted field-effect mobilities for the TFT devices are around 0.3 cm^2/V·s (Figure 1(c)), implying decent electron transport properties of the ZnO interlayers.

We then fabricated inverted OPVs according to standard procedures. The device structure is depicted in Figure 2(a). A solution of P3HT: PCBM (15 mg/ml, 1:0.8 by weight) in 1,2-dichlorobenzene was spin cast on the ZnO film and the resulting active layer, ca. 100 nm in thickness, was annealed at 150 °C for 12 min in glove-box. Thin films of MoO_x (6 nm) and Al (100 nm) were deposited by thermal evaporation. The final active area of the devices was 7.25 mm^2. Devices with the conventional structure (ITO/PEDOT: PSS/active layer/Al) were also fabricated as references. All devices were tested without encapsulation under ambient conditions using a Keithley 2400 SMU and Newport Oriel xenon lamp (300 W) with an AM 1.5 filter. The light intensity was calibrated to 100 mW/cm^2. The inverted solar cells using the ZnO interlayers from the aqueous precursor solution exhibit efficiencies comparable to the reference devices with the conventional structure.[19] The device parameters, including open circuit voltage (V_{OC}), short circuit current density (J_{SC}), fill factor (FF), and power conversion efficiency (PCE), are summarized in Figure 2(b) and Table I. For the inverted devices, a highest PCE of 4.17% and an average PCE of 3.93% were obtained. The stability of the inverted devices is significantly improved due to the use of metal oxides on both sides of the active layer: the PCE remained above 80% of the original value after 30 days. In contrast, for the reference cells with the conventional structure, the PCE decreased by a factor of 2 after 24 h.

We carried out studies associated with UV-ozone treatment on the ZnO thin films, aiming to gain more insights on the critical factors that control the properties of the electron transport interlayer and the overall device performance. The annealed ZnO thin films were subjected to UV-ozone for 15 min. UPS measurements indicate that such a treatment resulted in an increase of 0.6 ± 0.1 V in the work function of the interlayers (Figure 3(a)). We note that Olson and coworkers have also reported an increase of work function of the planar ZnO sol-gel films due to UV-ozone treatment.[20] The UV-ozone treatment also slightly altered the wetting properties of the ZnO interlayers. The contact angles of water on the ZnO films were decreased from 48° to 34° after the treatment (Figure S1).[23] The surface roughness of the ZnO thin films was not greatly affected by the UV-ozone treatment as indicated by the RMS value (from 2.4 nm to 2.5 nm) from the AFM measurements (Figure S2). The devices with the ZnO interlayers treated by UV-ozone display inferior photovoltaic performance, as indicated by Figures 3(b), S3, and Table I. Most notable, the V_{OC} is 120 mV lower compared to the cells with the ZnO interlayers that were not treated by UV-ozone.

We suggest that the work function of the ZnO electron transport interlayer is critical for the photovoltaic performance

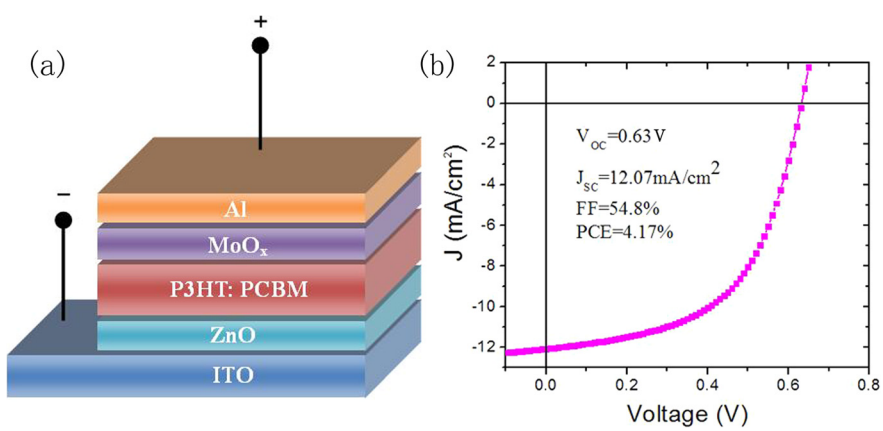

FIG. 2. (a) Schematic view of the structure of the inverted solar cell. (b) J-V curve of the champion device.

TABLE I. Photovoltaic performance of the inverted solar cells and the reference devices.

Device	V_{OC} (V)	J_{SC} (mA/cm^2)	*FF* (%)	Average *PCE* (%)	Best *PCE* (%)
ZnO without UV-ozone treatment	0.63	9.99	62.4	3.93	4.17
ZnO treated by UV-ozone	0.51	9.25	48.2	2.27	2.35
Reference device	0.61	9.03	63.2	3.48	3.62

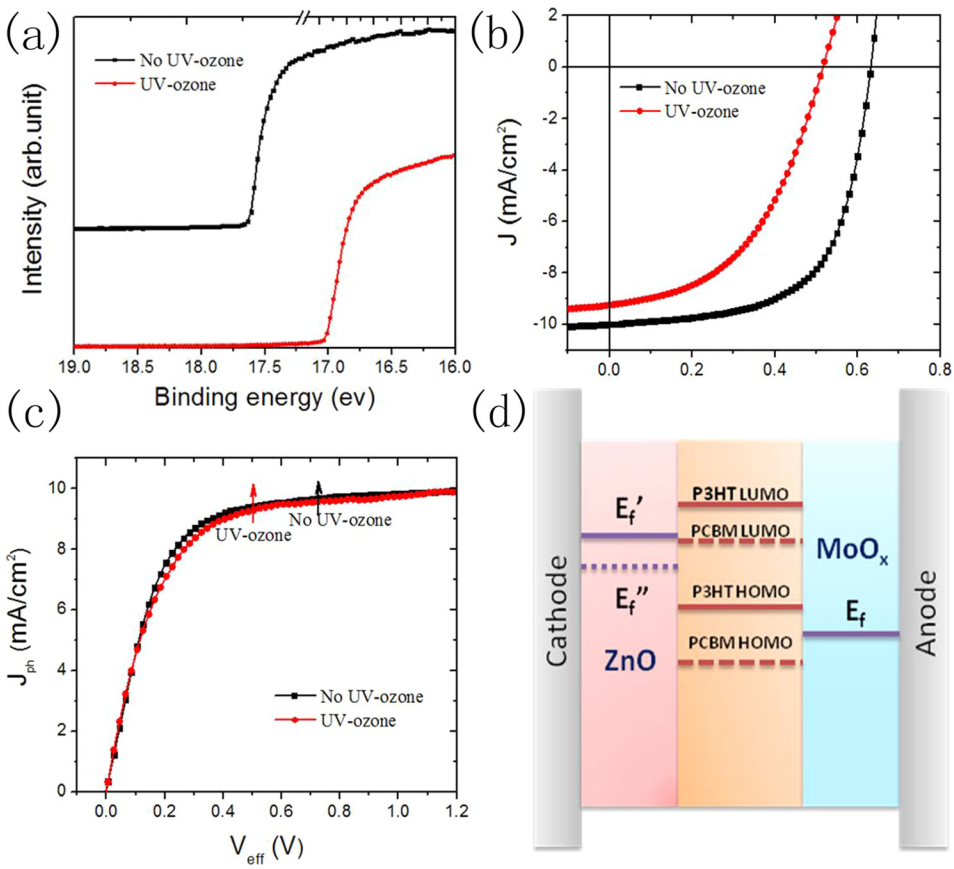

FIG. 3. Effects of UV-ozone treatments on the ZnO interlayers. (a) UPS spectra of annealed ZnO film with (black squares) or without UV-ozone treatments (red circles). (b) J-V curves and (c) J_{ph}-V_{eff} curves for inverted solar cells using ZnO interlayers with (red circles) and without (black squares) UV-ozone treatments. The arrows in (c) indicate the short-circuit photocurrent densities and the corresponding compensation voltages of the two devices. (d) Interfacial band alignment between ZnO interlayers and the photoactive layer before (solid line) and after (dashed line) UV-ozone treatment.

of the inverted solar cells. This deduction is supported by the plotting of net photocurrent (J_{ph}) against effective voltage (V_{eff}), which illustrates the dependence of photocurrent on the internal electric field.[21,22] J_{ph} is recorded by subtracting the dark current from the current under illumination. V_{eff}, which reflects the internal field in the device, is defined as $V_{eff} >= V_0 - V$, in which V_0 is the compensation voltage determined from the corresponding $J_{ph} - V$ curve (Figure S4). As shown in Figure 3(c), despite of the striking differences of V_{OC}, J_{SC}, and *FF*, the effects of UV-ozone treatments on photocurrent is minimal when scaled against V_{eff}. Note that UV-ozone treatments lead to ZnO interlayers with different surface wetting properties, which may influence the subsequent deposition of photoactive layer. We suggest that this issue is a minor factor that accounts for the changes of the photovoltaic performance of the cells considering the small discrepancy of the corresponding $J_{ph} - V_{eff}$ curves in Figure 3(c). The most critical factor is the increase in the work function of the ZnO interlayers which results in a smaller built-in potential and in consequence changes the internal electric field of the devices, as depicted in Figure 3(d). Since the processes of charge recombination and charge transport in the photoactive layer are electric field dependent,[4] we conclude that the observed changes in V_{OC}, J_{SC}, and *FF* are mainly due to the modification of the work function of the ZnO interlayer.

In conclusion, we developed a facile solution processable and low temperature ($\leq$150 °C) approach to deposit ZnO electron transport interlayers for the inverted organic solar cells by taking advantage of the stable and non-toxic aqueous precursor solutions of ammine-hydroxo zinc complex, $[Zn(NH_3)_x](OH)_2$. We fabricated inverted P3HT/PCBM solar cells, which exhibit decent efficiencies and stability, by using ZnO electron transport interlayers from the aqueous precursor solution. We studied the effects of UV-ozone treatments on the ZnO thin films and concluded that the work function of the electron transport interlayers was critical in terms of determining the photovoltaic performance of the inverted devices. The results define a promising approach for the fabrication of high quality electron transport interlayer of the inverted organic solar cells at low temperatures.

We would like to thank National Natural Science Foundation of China (51172203, 60906039), National High Technology Research and Development Program of China (2011AA050520), Natural Science Funds for Distinguished Young Scholar of Zhejiang Province (R4110189), the

Program for New Century Excellent Talents in University, and the Program for Professor of Special Appointment (Eastern Scholar) at Shanghai Institutions of Higher Learning for the financial support. We thank Dr. Jianpu Wang and Dr. Feng Gao (University of Cambridge, UK) for many inspiring discussions.

[1]J. Y. Kim, K. Lee, N. E. Coates, D. Moses, T. Q. Nguyen, M. Dante, and A. J. Heeger, Science **317**(5835), 222 (2007).
[2]G. Yu, J. Gao, J. C. Hummelen, F. Wudl, and A. J. Heeger, Science **270**(5243), 1789 (1995).
[3]C. R. McNeill, A. Abrusci, J. Zaumseil, R. Wilson, M. J. McKiernan, J. H. Burroughes, and R. H. Friend, Appl. Phys. Lett. **90**, 193506 (2007).
[4]P. W. M. Blom, V. D. Mihailetchi, L. J. A. Koster, and D. E. Markov, Adv. Mater. **19**(12), 1551 (2007).
[5]R. F. Service, Science **332**(6027), 293 (2011).
[6]M. Jorgensen, K. Norrman, and F. C. Krebs, Sol. Energy Mater. Sol. Cells **92**(7), 686 (2008).
[7]K. Kawano, R. Pacios, D. Poplavskyy, J. Nelson, D. D. C. Bradley, and J. R. Durrant, Sol. Energy Mater. Sol. Cells **90**(20), 3520 (2006).
[8]G. Li, C. W. Chu, V. Shrotriya, J. Huang, and Y. Yang, Appl. Phys. Lett. **88**(25), 253503 (2006).
[9]M. Jorgensen, K. Norrman, S. A. Gevorgyan, T. Tromholt, B. Andreasen, and F. C. Krebs, Adv. Mater. **24**(5), 580 (2012).
[10]M. S. White, D. C. Olson, S. E. Shaheen, N. Kopidakis, and D. S. Ginley, Appl. Phys. Lett. **89**(14), 143517 (2006).
[11]S. K. Hau, H.-L. Yip, N. Seob Baek, J. Zou, K. O'Malley, and A. K. Y. Jen, Appl. Phys. Lett. **92**(25), 253301 (2008).
[12]P. de Bruyn, D. J. D. Moet, and P. W. M. Blom, Org. Electron. **11**(8), 1419 (2010).
[13]Y. Sun, J. Hwa Seo, C. J. Takacs, J. Seifter, and A. J. Heeger, Adv. Mater. **23**(14), 1679 (2011).
[14]J.-C. Wang, W.-T. Weng, M.-Y. Tsai, M.-K. Lee, S.-F. Horng, T.-P. Perng, and H.-F. Meng, J. Mater. Chem. **20**(5), 862 (2010).
[15]B. N. Illy, A. C. Cruickshank, S. Schumann, R. Da Campo, T. S. Jones, S. Heutz, and M. P. Ryan, J. Mater. Chem. **21**(34), 12949 (2011).
[16]A. K. K. Kyaw, X. W. Sun, C. Y. Jiang, G. Q. Lo, D. W. Zhao, and D. L. Kwong, Appl. Phys. Lett. **93**(22), 221107 (2008).
[17]C. E. Small, S. Chen, J. Subbiah, C. M. Amb, S.-W. Tsang, T.-H. Lai, and F. So, Nature Photon. **6**(2), 115 (2012).
[18]S. T. Meyers, J. T. Anderson, C. M. Hung, J. Thompson, J. F. Wager, and D. A. Keszler, J. Am. Chem. Soc. **130**(51), 17603 (2008).
[19]Z. Wu, T. Song, Y. Jin, and B. Sun, Appl. Phys. Lett. **99**(14), 143306 (2011).
[20]D. C. Olson, Y.-J. Lee, M. S. White, N. Kopidakis, S. E. Shaheen, D. S. Ginley, and J. W. P. Hsu, J. Phys. Chem. C **112**(26), 9544 (2008).
[21]V. D. Mihailetchi, L. J. A. Koster, and P. W. M. Blom, Appl. Phys. Lett. **85**(6), 970 (2004).
[22]M. Lenes, M. Morana, C. J. Brabec, and P. W. M. Blom, Adv. Funct. Mater. **19**(7), 1106 (2009).
[23]See supplementary material at http://dx.doi.org/10.1063/1.4719201 for contact angle measurements of the ZnO films (Figure S1), Surface features of the ZnO films (Figure S2), EQE curves of the inverted cells using ZnO interlayers (Figure S3), and J_{ph} – V curves derived from Figure 3(b) (Figure S4).